INFLUENCE OF EPOXY- AND POLYAMIDE-COMPATIBLE CARBON FIBER SIZINGS ON INTERFACIAL FRACTURE TOUGHNESS AND IN-PLANE SHEAR PROPERTIES OF CARBON FIBER REINFORCED POLYAMIDE-6

M. Greisel[1], A. Kurek[2], A. Chaloupka[3], J. Moosburger-Will[4], W.M. Mueller[1], M.G.R. Sause[1] and S. Horn[1,4]

[1]Experimental Physics II, Institute of Physics, University of Augsburg, 86135 Augsburg, Germany
Email: michael.greisel@physik.uni-agusburg.de
Web Page: http://www.physik.uni-augsburg.de/en/lehrstuehle/exp2
[2]SGL Carbon GmbH, 86405 Meitingen, Germany
[3]Branch Functional Lightweight Design, Fraunhofer ICT, 86159 Augsburg, Germany
[4]Institute of Materials Resource Management, University of Augsburg, 86135 Augsburg, Germany

Keywords: thermoplastic composites, carbon fiber sizing, single-fiber push-out test, in-plane shear

Abstract
The fiber-matrix interaction is one of the key parameters to optimize the mechanical performance of fiber reinforced polymers. For this purpose, a sufficiently strong adhesion between fiber and matrix is necessary. This can be accomplished by employing a suitable polymeric sizing. Since conventional sizing agents, designed for thermoset composites, are usually chemically incompatible with thermoplastic matrices and do not withstand their higher processing temperatures, new customized sizings are required. In the present study, the effects of a conventional epoxy-compatible sizing and two polyamide-compatible sizing agents on micro- and macro-mechanical properties of carbon fiber reinforced polyamide-6 were investigated. On a microscopic scale, cyclic single-fiber push-out tests were performed to evaluate the interfacial fracture toughness. To determine the macro-mechanical in-plane shear properties, V-notched rail shear and picture frame tests were performed. Results of microscopic push-out and macroscopic shear tests are consistent and reveal highest level of adhesion to the matrix for one of the polyamide-compatible sizings. The sample with epoxy-compatible sizing shows the lowest value of fiber-matrix adhesion. It is concluded that the customized, matrix-compatible sizing improves the fiber-matrix adhesion on microscopic scale, which in turn improves the in-plane shear properties on macroscopic scale.

1. Introduction

Thermoplastic polymer based composites (TPCs) are currently receiving considerable attention due to time-saving and flexible production processes compared to thermoset composites. Long shelf life of the matrix, weldability, high fracture toughness and recyclability of the composite are further advantages. Since the mechanical properties of fiber reinforced composites are closely related to the fiber-matrix interaction, the benefits of TPCs can only be reached in composites with a strong adhesion between carbon fiber and thermoplastic matrix. A variety of methods and improvements to tailor the interfacial properties, e.g. plasma treatment or nanoparticles coating of carbon fibers, are summarized in recent reviews [1, 2].

State of the art in industrial carbon fiber manufacturing is the application of a polymeric sizing to the carbon fibers after the electrolytic surface activation. Main functions of the sizing are to protect the

fibers from surface damages during the textile processes as well as to improve the handling of the fiber bundles and the wetting of carbon fibers by the matrix polymer [3–6]. In addition, the sizing is applied to accomplish a strong interaction between fiber and matrix [2–4, 7, 8]. Decisive factor for good adhesion is the chemical compatibility between the sized fiber surface and the matrix material [2, 3, 5]. However, due to the high proportion of epoxy-based composites in composite applications, most of the commercially available sizing materials are compatible to epoxy rather than thermoplastic matrices [2, 5, 9]. Besides the lack of chemical interaction, epoxy-compatible sizings already start to degrade at temperatures below the processing temperatures of TPCs. Thus, new sizings tailored for thermoplastics are required that fulfill the demands of chemical compatibility to the matrix and that ensure thermal stability up to the melting region of the thermoplastic polymer matrix.

In the present study, the influence of a conventional epoxy-compatible sizing and two polyamide-compatible sizings on the micro- and macro-mechanical quantities of carbon fiber reinforced polyamide-6 (PA6) composites is presented. On microscopic scale, cyclic single-fiber push-out tests were conducted to evaluate the interfacial fracture toughness. To determine the macro-mechanical in-plane shear properties, V-notched rail shear (VNRS) and picture frame (PF) tests were performed.

2. Experimental

2.1. Materials

The samples investigated in the present study are unidirectional carbon fiber reinforced polyamide-6 matrix composites. For the production of test panels, preimpregnated C/PA6-tapes with uniaxial orientated fibers of varying sizing were available. In three tapes of R&D grade, an epoxy-compatible suspension (EP) and two polyamide-compatible sizings (TP0 and TP1) were applied to the fibers, respectively. The fourth tape is a product of commercial grade with an unknown sizing (REF). Precise layup of the tapes was accomplished by an automated tape laying process (Relay 2000, Fiberforge). Due to varying thickness of the tapes, different amounts of plies were necessary to produce the nominal thickness of the required test plates. The stacking sequences of the individual panels for the three test procedures are given in Table 1.

Table 1: Layup of the different UD-laminates.

Material system	Layup Push-out Test (2mm)	Layup VNRS-Test (3mm)	Layup PF-Test (4mm)
C/PA6-EP	$[0]_{12}$	$[0]_{18}$	$[0]_{24}$
C/PA6-TP0	$[0]_{12}$	$[0]_{18}$	$[0]_{24}$
C/PA6-TP1	$[0]_{9}$	$[0]_{14}$	$[0]_{16}$
C/PA6-REF	$[0]_{14}$	$[0]_{22}$	$[0]_{32}$

All layups were dried in an oven at 80 °C for at least 6 hours. After drying, each stack was heated on a contact heater to 265 °C, subsequently transferred in a press already heated to 80 °C and finally pressed at 50 bar. After keeping pressure constant for 90 s, the press was opened and the laminate was cooled down pressurelessly to room temperature.

2.2. Sample preparation

For the push-out tests, thin slices of about 10 mm x 2.0 mm x 0.7 mm were cut by a diamond saw (Isomet, Buehler) and thinned to an appropriate thickness by a two-sided lapping and polishing process (PM5, Logitech Ltd.). Plane-parallel sample surfaces were generated with minimal damage to the sample and with the fiber axis direction being parallel aligned to the thickness direction of the slices. According to this procedure, up to three push-out samples with different thicknesses were produced for each C/PA6-system. An overview of the samples prepared is given in Table 2. In the next step, the

thinned slices were placed on glass substrates with a groove of typically 60 µm in width. The setting by quartz wax ensured a close and stiff contact to the substrate.

Table 2: Overview of prepared push-out specimens.

	Specimen	C/PA6-EP	C/PA6-TP0	C/PA6-TP1	C/PA6-REF
Specimen thickness (µm)	1	24.4 ± 1.0	24.2 ± 0.9	25.4 ± 0.8	27.8 ± 1.0
	2	36.1 ± 1.4	34.0 ± 1.2	35.4 ± 1.0	38.6 ± 1.1
	3	45.8 ± 1.2	44.6 ± 1.0	45.8 ± 1.3	-

For VNRS-tests, rectangular test specimens with nominal dimensions of 76 mm x 56 mm and centrally located V-notches were separated from the laminates by water jet cutting according to the specifications of ASTM D7078 [10]. During pretests all specimens failed by vertical cracking starting at the top or bottom edge in the clamping regions. To induce higher shear forces in the gage section, a higher notch-effect was sought. Therefore, the width of the notch was increased from 25.4 mm to 28.5 mm and the depth from 12.7 mm to 14.3 mm. Notch angle (90°) and tip radius (1.3 mm) remained unchanged. The fiber axis was oriented parallel to the applied shear strain to determine in-plane shear properties.

The test coupons for the PF-test were milled according to the specifications given in Ref. [11]. Quadratic specimens with nominal dimensions of 165 mm x 165 mm and a free shear area of 105 mm x 105 mm were prepared with corner-cuts and drillings in the clamping range. The fibers are again oriented in shear strain direction to obtain in-plane shear properties.

2.3. Test setups and procedure

During a single-fiber push-out test, an individual fiber is loaded by a rigid indenter tip with increasing compressive load resulting in fiber-matrix debonding and fiber push-out. The tests were performed at room temperature using an Universal Nanomechanical Tester (Asmec GmbH), which allows displacement-controlled measurements in normal direction with an accuracy of 0.01 mN and 1 nm, respectively. In lateral direction, the positioning accuracy of the indenter tip is 1µm. In the present study, the push-out tests were performed with a flat-end indenter tip of cylindrical shape (diameter at the tip of 5.3 µm). The push-out tests were conducted using a cyclic loading schedule, published in recent push-out studies [12–15]. The cyclic loading schedule consists of subsequent unloading-reloading cycles in regular steps of 100 nm or 200 nm up to a maximum indenter displacement of 6.0 µm. The loading/ unloading segments were performed at a displacement rate of 100 nm/s. The individually tested fibers were chosen randomly irrespective of the local fiber volume content of the measurement position. A number of at least 20 fibers of comparable cross-section area were tested for each push-out sample. Based on this random selection, the results are assumed to represent the interfacial properties and failure behavior of the whole sample. Prior to testing, the specimens were conditioned according to Ref. [16].

An energy analysis of the push-out test adapted for ductile matrix systems [12–15] was used to evaluate the interfacial fracture toughness. The average fracture toughness $\langle G \rangle$ is calculated according to Eq. 1.

$$\langle G \rangle = -\frac{\Delta E_{\mathrm{crack,stable}}}{\Delta A_{\mathrm{crack,stable}}} \tag{1}$$

The energy contribution $\Delta E_{\mathrm{crack,stable}}$ is determined by the cyclic push-out test, as presented in Refs [13–15]. The corresponding fracture surface area of stable crack growth $\Delta A_{\mathrm{crack,stable}}$ is quantified according to a new approach presented by Mueller et al. [17]. This model for stable and unstable crack propagation allows to quantify the relevant crack area on the basis of a linear relationship between the total energy dissipated during stable crack propagation and the sample thickness (see Eq. 2). The model was verified experimentally in Refs. [13, 15, 17].

$$-\frac{\Delta E_{\mathrm{crack,stable}}}{U_{\mathrm{F}}} = \langle G \rangle \cdot (L - L_{\mathrm{unst}}) \tag{2}$$

with circumference of the fiber U_{F}, sample thickness L and length of unstable crack growth L_{unst}.

The VNRS-tests were performed in an universal testing machine (Zmart.Pro, Zwick Roell) at room temperature with a crosshead speed of 2 mm/min. The displacement field on one side of each specimen was measured through 2D digital image correlation (Aramis 12M, GOM). To this end, a speckle pattern is sprayed on the specimen surface. Images with a resolution of 4096 pixel x 3072 pixel, a focal length of 50 mm and a lens speed of f/2.8 were captured with a frequency of 2 Hz. The local strain values were calculated with a facet size of 19 pixel x 19 pixel. For evaluation of the shear strain, the mean value of a rectangular strain field of 3 mm x 24 mm at the center of the specimen surface was calculated. Before testing started, the specimens were conditioned according to Ref. [16].

The PF-tests were conducted in an universal testing machine (Z250, Zwick/Roell) with a crosshead speed of 4 mm/min up to a maximum crosshead travel of 24 mm [11]. The deformation was measured using a 3D digital image correlation (DIC) system (Aramis 12M, GOM). The specimens were conditioned according to [16] and a black-on-white speckle pattern was applied on the surface of each specimen. The images were captured with a frequency of 1 Hz at a focus length of 100 mm and a lens speed of f/5.6. To evaluate the shear strain, the mean value of a rectangular strain field of 5 mm x 10 mm with a 45°-orientation to the fiber axis at the center of the specimen was calculated.

3. Results and Discussion

3.1. Cyclic single-fiber push-out tests

In Fig. 1(a), a representative load-displacement diagram of a cyclic single-fiber push-out test, performed on a C/PA6 composite is presented. After a linear increase of the envelope curve up to an indenter displacement of about 0.2 µm, deviation from linear increase until peak load is observed. After the maximum, the load decreases over several cycles up to a displacement of around 3.8µm. Here, the sign of the curvature changes again and leads up to a progressive push-out behavior at a nearly constant load level (around 13 mN) for the following loading cycles. Since the excess elastic energy stored in the fiber is dissipated by work of friction during slipping of the debonded fiber against the surrounding matrix, no abrupt fiber push-out occurs [15].

The total dissipated plastic deformation energy increases linearly as a function of the indenter displacement (Fig. 1(b)) over a broad region. This stable energy consuming process is attributed to stable crack propagation [13, 14]. Back-extrapolation of the linear regression to zero dissipated energy yields the crack initiation point. For progressive push-out failure, deviation from linearity of the total plastic energy occurs at the onset of constant load level (Fig. 1(a)). The deviation from linearity can be regarded as the endpoint of stable crack propagation and the transition to frictional slipping [15]. Thus, the stable crack energy is equal to the difference in energy between the crack initiation point and the point of deviation from linearity, as denoted in Fig. 1(b).

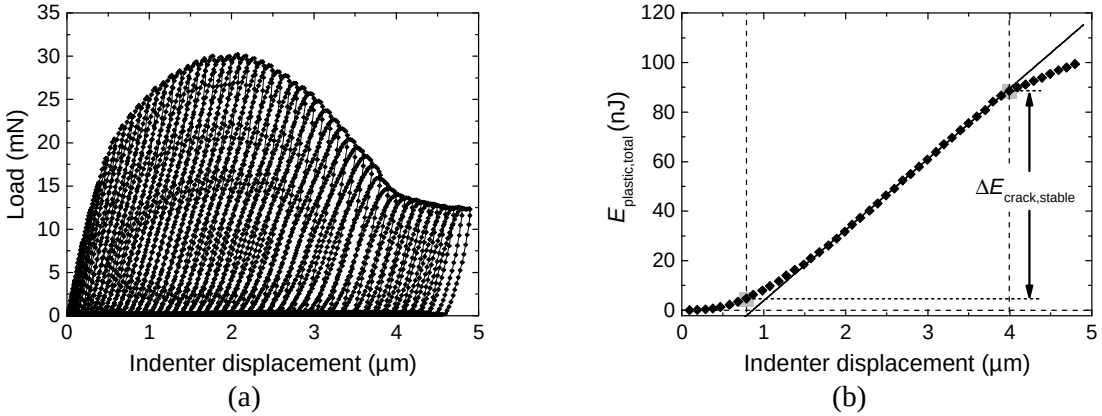

Figure 1. Representative load-displacement diagram of a cyclic single-fiber push-out test performed on C/PA6 (a) and corresponding total plastic energy dissipated during progressive push-out process as a function of indenter displacement (b).

To evaluate the interfacial fracture toughness, cyclic push-out tests were performed on the specimens listed in Tab. 2 and individual crack energies were evaluated for each sample thickness. In Fig. 2(a), the mean $\Delta E_{\mathrm{crack,stable}}$ - normalized to the individual fiber circumference - is plotted for the examined samples. All data points can be approximated by a linear regression according to Eq. (2), which confirms the model of Mueller et al. [17]. The slopes of the linear regressions yield the interfacial fracture toughness of the individual C/PA6-material systems. For comparison, the values are plotted in Fig. 2(b).

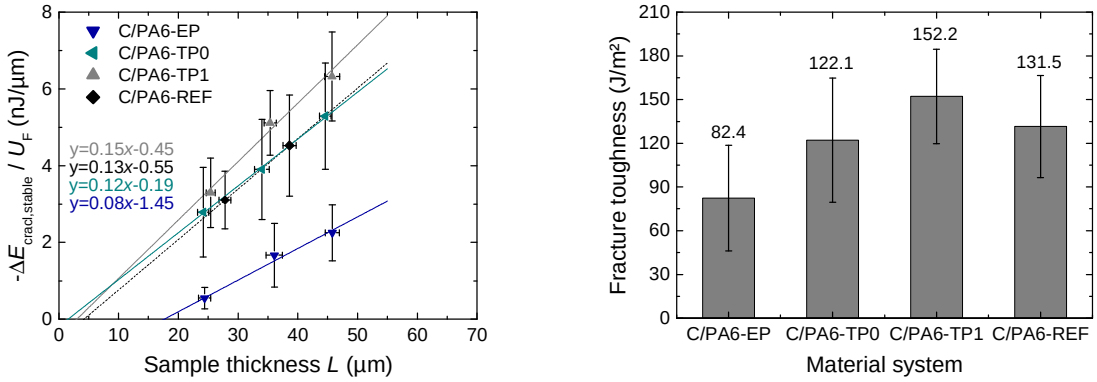

(a) (b)

Figure 2. Diagram of the energy dissipated by stable crack propagation as a function of sample thickness (a). The slopes of the linear regressions yield the interfacial fracture toughness $\langle G \rangle$ of the individual C/PA6-systems according to Eq. (2) (b).

The results of push-out tests reveal clear differences in the mean values of interfacial fracture toughness between the samples with polyamide-compatible sizing (C/PA6-TP0 and C/PA6-TP1) and the sample with the epoxy-compatible sizing (C/PA6-EP). C/PA6-EP yields the lowest interfacial fracture toughness. Compared to C/PA6-REF, the mean value of C/PA6-EP is 37 % smaller. The mean fracture toughness of C/PA6-TP0 is merely 7 % smaller and the mean value of C/PA6-TP1 is higher by 16 %. Thus, highest level of fiber-matrix interaction is achieved for sizing TP1.

3.2. In-plane shear tests

The failure mode intended for VNRS-tests with the fibers (1-axis) parallel oriented to the applied shear strain is a mode-II dominated vertical crack in the gage section between the notch tips (Fig. 3(a), left). Although the notch-effect on the test coupons was increased in this study, mode-I dominated cracking in the side edges of the notches often occurs. This can be attributed to setup-induced transversal strains, as measured by DIC and shown in Fig. 3(a), right.

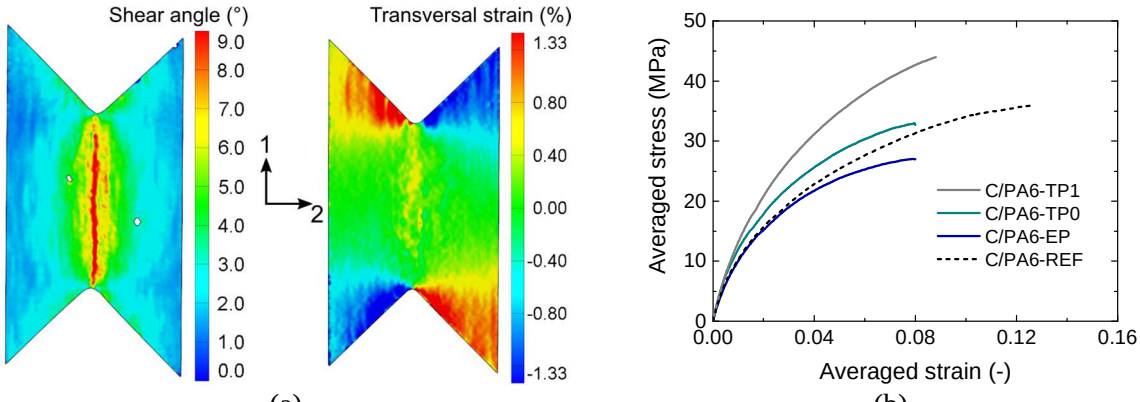

(a) (b)

Figure 3. Strain signatures obtained by digital image correlation during the VNRS-tests (a) and averaged stress-strain curves (b).

The transverse tension in the top left and the bottom right side edges (red color-coding) tends to induce cracking along intrinsic flaws, e.g. pores, dry fiber bundles, gaps between the tapes and matrix-rich zones within the coupon samples. In addition, a significant transversal strain in the gage section is detected. Thus, no pure intralaminar shear stress state is reached with this test procedure and failure of the specimens is determined by a superimposed stress state of intralaminar shear and transverse tensile stress. Therefore, the VNRS-tests only allow for qualitative evaluation of the influence of the sizing agent. In Fig. 3(b), the averaged stress-strain curves of the tests are shown. Comparing the averaged curves, C/PA6-TP1 withstands the highest combined stress level followed by C/PA6-REF and C/PA6-TP0. C/PA6-EP withstands lowest stress. Hence, the order of the material systems concerning their maximum stress level confirms the tendencies also found in push-out testing.

Loading of the test coupons in the PF-test causes pure shear deformation without transverse strain components [18]. Due to the clamping and loading principle, a maximum shear load is caused in the middle of the specimen. This is taken into account by correction factors for the determination of shear modulus and strength [11, 18]. However, during shear loading of the laminates with varying sizing agents, additional strain maxima were detected by DIC measurements in off-center positions. These local maxima sometimes induced primary failure. This again is attributed to intrinsic flaws, present in the test plates investigated. In such cases, the shear strength was calculated by the mean shear stress acting within the shear area of the coupons. In Fig. 4, the determined shear strength values are presented.

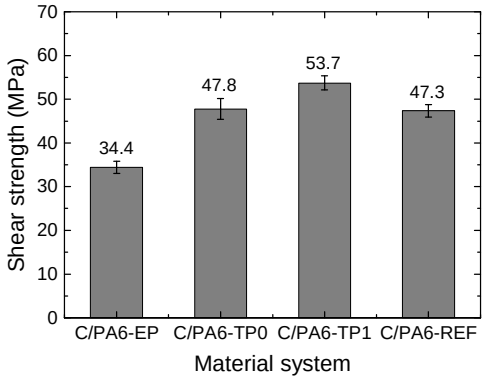

Figure 4. Comparison of the shear strength obtained by PF-testing.

Results of PF-tests also reveal clear differences between the samples with polyamide-compatible sizing and the sample with the epoxy-compatible sizing. Compared to the reference, the shear strength of C/PA6-EP is 27 % lower. While the shear strength of C/PA6-TP0 is nearly equal to C/PA6-REF, the shear strength of C/PA6-TP1 is higher by 14 %. This result is in agreement with the finding of the VNRS-tests. In consequence, the fracture toughness as determined from micro-mechanical push-out tests shows the same trend as macro-mechanical in-plane shear tests.

4. Conclusions

The present work demonstrates the effect of epoxy- and polyamide-compatible sizings in carbon fiber reinforced polyamide-6 composites on the micro-mechanical fracture toughness and the macro-mechanical in-plane shear properties. Results gained from single-fiber push-out, V-notched rail shear and picture frame tests reveal consistent tendencies and improved micro- and macro-mechanical properties, when a matrix-compatible sizing is applied. This suggests that strong adhesion via chemical and/or hydrogen bonds between the PA6 matrix and the carbon fibers with polyamide-compatible sizing can be achieved. Obviously, the epoxy-compatible sizing cannot form such strong adhesion, which is attributed to weak intermolecular bondings, e.g. van der Waals forces. In summary, we have shown that the chemical compatibility between sizing and matrix is a decisive parameter that can deeply affect the mechanical performance.

Acknowledgments

The authors would like to thank the German Federal Ministry for Education and Research (BMBF) for funding the project MAI Polymer within the Leading-Edge Cluster MAI Carbon.

References

[1] Karger-Kocsis, J., Mahmood, H., and Pegoretti, A. Recent advances in fiber/matrix interphase engineering for polymer composites. *Progress in Materials Science*, 73:1–43, 2015.
[2] Sharma, M., Gao, S., Mäder, E., Sharma, H., Wei, L. Y., and Bijwe, J. Carbon fiber surfaces and composite interphases. *Composites Science and Technology*, 102:35–50, 2014.
[3] Thomason, J. L. and Adzima, L. J. Sizing up the interphase: an insider's guide to the science of sizing. *Composites Part A: Applied Science and Manufacturing*, 32(3–4):313–321, 2001.
[4] Yuan, H., Zhang, S., Lu, C., He, S., and An, F. Improved interfacial adhesion in carbon fiber/polyether sulfone composites through an organic solvent-free polyamic acid sizing. *Applied Surface Science*, 279(0):279–284, 2013.
[5] Yuan, H., Zhang, S., and Lu, C. Surface modification of carbon fibers by a polyether sulfone emulsion sizing for increased interfacial adhesion with polyether sulfone. *Applied Surface Science*, 317:737–744, 2014.
[6] Upadhyaya, D. and Tsakiropoulos, P. Evaluation of the effect of sizing levels on transverse flexural and shear strengths of carbon/epoxy composites. *Journal of Materials Processing Technology*, 54(1–4):17–20, 1995.
[7] Drzal, L. T. and Raghavendran, V. K. Adhesion of Thermoplastic Matrices to Carbon Fibers: Effect of Polymer Molecular Weight and Fiber Surface Chemistry. *Journal of Thermoplastic Composite Materials*, 16((1):21–30, 2003.
[8] Karsli, N. G., Ozkan, C., Aytac, A., and Deniz, V. Effects of sizing materials on the properties of carbon fiber-reinforced polyamide 6,6 composites. *Polymer Composites*, 34(10):1583–1590, 2013.
[9] Yumitori, S., Wang, D., and Jones, F. R., 1994. The role of sizing resins in carbon fibre-reinforced polyethersulfone (PES). *Composites Part A: Applied Science and Manufacturing*, 25(7) (1994):698–705.
[10] ASTM Standard D7078/D7078M-05. *Standard Test Method for Shear Properties of Composite Materials by V-Notched Rail Shear Method*. ASTM International, West Conshohocken PA, 2005.
[11] DIN SPEC 4885. *Faserverstärkte Kunststoffe – Schubversuch mittels Schubrahmen zur Ermittlung der Schubspannungs-/Schubverformungskurve und des Schubmoduls in der Lagenebene*. Beuth Verlag GmbH, Berlin, 2014.
[12] Battisti, A., los Ojos, D. E.-d., Ghisleni, R., and Brunner, A. J. Single fiber push-out characterization of interfacial properties of hierarchical CNT-carbon fiber composites prepared by electrophoretic deposition. *Composites Science and Technology*, 95(0):121–127, 2014.
[13] Greisel, M., Jäger, J., Moosburger-Will, J., Sause, M., Mueller, W., and Horn, S. Influence of residual thermal stress in carbon fiber-reinforced thermoplastic composites on interfacial fracture toughness evaluated by cyclic single-fiber push-out tests. *Composites Part A: Applied Science and Manufacturing*, 66:117–127, 2014.
[14] Jäger, J., Sause, M. G. R., Burkert, F., Moosburger-Will, J., Greisel, M., and Horn, S. Influence of plastic deformation on single-fiber push-out tests of carbon fiber reinforced epoxy resin. *Composites Part A: Applied Science and Manufacturing*, 71(0):157–167, 2015.
[15] Greisel, M., Jäger, J., Moosburger-Will, J., Sause, M., Mueller, W., and Horn, S. Evaluation of the interfacial fracture toughness of a carbon fiber reinforced thermoplastic composite by cyclic single-fiber push-out tests. *Proceedings of the 20th International Conference on Composite Materials ICCM-20*, Kopenhagen, Dänemark, 2015.
[16] DIN EN ISO 1110. *Polyamides - Accelerated conditioning of test specimens*. Beuth Verlag GmbH, Berlin, 1998.

[17] Mueller, W. M., Moosburger-Will, J., Sause, M. G. R., Greisel, M., and Horn, S. Quantification of crack area in ceramic matrix composites at single-fiber push-out testing and influence of pyrocarbon fiber coating thickness on interfacial fracture toughness. *Journal of the European Ceramic Society*, 35(11):2981–2989, 2015.
[18] Basan, R. *Untersuchung der intralaminaren Schubeigenschaften von Faserverbundwerkstoffen mit Epoxidharzmatrix unter Berücksichtigung nichtlinearer Effekte*. BAM-Dissertationsreihe (Band 74). Bundesanstalt f. Materialforschung und -prüfung, Berlin, 2011.